Cellular/Molecular

Muscarinic Enhancement of R-Type Calcium Currents in Hippocampal CA1 Pyramidal Neurons

Chao Tai,[1]***J. Brent Kuzmiski,**[1,2]* **and Brian A. MacVicar**[1]

[1]Brain Research Center, Department of Psychiatry, University of British Columbia, Vancouver, British Columbia V6T 2B5, Canada, and [2]Hotchkiss Brain Institute, Calgary, Alberta T2N 4N1, Canada

The "toxin-resistant" R-type Ca^{2+} channels are expressed widely in the CNS and distributed mainly in apical dendrites and spines. They play important roles in regulating signal transduction and intrinsic properties of neurons, but the modulation of these channels in the mammalian CNS has not been studied. In this study we used whole-cell patch-clamp recordings and found that muscarinic activation enhances R-type, but does not affect T-type, Ca^{2+} currents in hippocampal CA1 pyramidal neurons after N, P/Q, and L-type Ca^{2+} currents selectively were blocked. M_1/M_3 cholinergic receptors mediated the muscarinic stimulation of R-type Ca^{2+} channels. The signaling pathway underlying the R-type enhancement was independent of intracellular $[Ca^{2+}]$ changes and required the activation of a Ca^{2+}-independent PKC pathway. Furthermore, we found that the enhancement of R-type Ca^{2+} currents resulted in the *de novo* appearance of Ca^{2+} spikes and in remarkable changes in the firing pattern of R-type Ca^{2+} spikes, which could fire repetitively in the theta frequency. Therefore, muscarinic enhancement of R-type Ca^{2+} channels could play an important role in modifying the dendritic response to synaptic inputs and in the intrinsic resonance properties of neurons.

Key words: acetylcholine; muscarinic; R-type calcium spikes; α1E calcium subunits; Ca_V2.3; T-type calcium currents; theta; epilepsy; oscillations; hippocampus

Introduction

R-type voltage-sensitive Ca^{2+} currents originally were identified as the high voltage-activated (HVA) Ca^{2+} currents that were resistant to the antagonists ω-conotoxin MVIIC, ω-conotoxin-GVIA, ω-agatoxin IVA, and the dihydropyridines (Zhang et al., 1993; Randall and Tsien, 1995). In hippocampal CA1 pyramidal neurons the R-type voltage-sensitive Ca^{2+} channels (VSCCs) are highly expressed in distal dendrites (Christie et al., 1995; Magee and Johnston, 1995) and are thought to be primarily responsible for Ca^{2+} influx in dendrites and spines (Sabatini and Svoboda, 2000; Yasuda et al., 2003). R-type Ca^{2+} currents are involved in generating action potential bursts and afterdepolarizations (Magee and Carruth, 1999; Metz et al., 2005) and in the induction of synaptic plasticity (Isomura et al., 2002; Breustedt et al., 2003; Dietrich et al., 2003; Yasuda et al., 2003).

Modulation of R-type Ca^{2+} currents could have profound impacts on dendritic excitability via modification of intrinsic firing patterns and the integrative properties of dendrites. Brief trains of backpropagating action potentials have been shown to depress Ca^{2+} entry through R-type VSCCs located in dendritic spines and thereby block theta burst-induced long-term potenti-

ation (LTP) (Yasuda et al., 2003). In expression systems the R-type Ca^{2+} currents caused by recombinant Ca_V2.3 (α1E) VSCCs (Piedras-Renteria and Tsien, 1998; Sochivko et al., 2002; Bannister et al., 2004) are stimulated by the activation of coexpressed muscarinic (Meza et al., 1999; Melliti et al., 2000; Bannister et al., 2004) or metabotropic glutamate receptors (mGluRs) (Stea et al., 1995). However, the modulation of R-type Ca^{2+} currents by muscarinic or metabotropic receptors has not been examined in native neurons in brain slices or *in vivo*. Therefore, we used whole-cell recordings to examine whether Ca^{2+} currents caused by R-type VSCCs are enhanced in hippocampal brain slices by muscarinic activation. We show that both R-type Ca^{2+} currents and spikes are enhanced by the stimulation of muscarinic receptors in CA1 pyramidal neurons. This is in striking contrast to the extensively studied depression of N-, P-/Q-, and L-type Ca^{2+} currents by the activation of muscarinic receptors (Gahwiler and Brown, 1987; Shapiro et al., 1999, 2001; Stewart et al., 1999). Furthermore, initiation of dendritic Ca^{2+} spikes has been suggested to play a role in generating or shaping neuronal network oscillations (Kamondi et al., 1998; Buzsaki, 2002). Interestingly, we found that muscarinic stimulation leads to remarkable and novel changes in the R-type Ca^{2+} spike firing pattern. After muscarinic receptor stimulation the enhanced R-type Ca^{2+} spikes repetitively fired at theta frequencies (6–10 Hz), and blocking R-type VSCCs depressed carbachol-induced spontaneous field potential theta oscillations, suggesting that enhanced R-type calcium spikes play a role in dendritic bursting and network oscillations. Therefore, muscarinic receptor activation in hippocampal neurons will alter profoundly the dendritic integration and intrinsic resonance properties by shifting the normal

pattern of Ca^{2+} entry from the slowly inactivating N-, P/Q-, and L-type VSCCs to domination by the HVA rapidly inactivating R-type VSCCs.

Materials and Methods

Hippocampal slice preparation. Hippocampal slices were prepared from Sprague Dawley rats, aged postnatal days 13–16, according to standard procedures (Fraser and MacVicar, 1996). Our experiments were approved by the Canadian Council for Animal Care and the University of British Columbia Animal Care Committee. All experiments were conducted in strict accordance with National Institutes of Health *Guide for the Care and Use of Laboratory Animals.* Briefly, the rats were anesthetized deeply with halothane and decapitated rapidly. The brain was removed quickly, and horizontal hippocampal slices ($\sim$400 μm) were cut with a vibratome (VT100, Leica, Willowdale, Ontario, Canada) in chilled (0–4°C) slicing solution containing the following (in mM): 75 sucrose, 87 NaCl, 25 NaHCO$_3$, 25 D-glucose, 2.5 KCl, 1.25 NaH$_2$PO$_4$, 0.5 CaCl$_2$, and 7.0 MgCl$_2$, pH 7.3. Then the slices were transferred to a storage chamber with fresh artificial CSF (ACSF) containing the following (in mM): 126 NaCl, 2.5 KCl, 2.0 MgCl$_2$, 2.0 CaCl$_2$, 1.25 NaH$_2$PO$_4$, 26 NaHCO$_3$, and 10 D-glucose, pH 7.3, and were incubated at room temperature for >1 h before recording. All solutions were saturated with 95% O$_2$/5% CO$_2$.

Whole-cell patch-clamp recordings. Whole-cell voltage-clamp or current-clamp recordings from CA1 neurons within hippocampal slices (Blanton et al., 1989) were obtained at room temperature (22–24°C). Individual slices were transferred to a recording chamber located on an upright microscope (Axioskop, Zeiss, Oberkochen, Germany) and perfused rapidly with oxygenated ACSF (2 ml/min). Patch electrodes (3–5 MΩ) were pulled from 1.5 mm outer diameter thin-walled glass capillaries (150F-4, World Precision Instruments, Sarasota, FL) in three stages on a Flaming-Brown micropipette puller (model P-97, Sutter Instruments, Novato, CA) and were filled with intracellular solution containing the following (in mM): 115 Cs-methanesulphonate, 25 TEA-Cl, 10 HEPES, 1.1 EGTA, 0.1 CaCl$_2$, 4 Mg-ATP, and 0.5 Na-GTP, pH 7.2. Intracellular $[Ca^{2+}]$ was calculated to be 16 nM. In some experiments BAPTA was substituted for EGTA, as described. In the BAPTA experiments stable whole-cell recordings were maintained for >15–20 min before recording to ensure that the BAPTA diffused into dendritic regions. R-/T-type Ca^{2+} currents were isolated pharmacologically by preincubating the slices in a mixture containing ω-conotoxin MVIIC (2 μM), ω-conotoxin-GVIA (2 μM), and ω-agatoxin IVA (0.4 μM) to block N-, P-, and Q-type Ca^{2+} currents and cytochrome c (0.1 mg/ml) to block nonspecific toxin binding for >1 h at room temperature. Nifedipine (20 μM) and tetrodotoxin (TTX; 1.2 μM) were bath applied to block L-type Ca^{2+} currents and Na$^+$ currents, respectively. Also, 2 mM CsCl and 1 mm 4-aminopyridine (4-AP) were bath applied to block residue K$^+$ channels.

Membrane potentials and currents were monitored with an Axopatch 200B amplifier (Molecular Devices, Union City, CA), acquired via a Digidata 1200 series analog-to-digital interface onto a Pentium computer with Clampex 9.0 software (Molecular Devices). Data were sampled at 10 kHz, and most were low-pass filtered (four-pole Bessel) at 1 kHz. Data were not filtered for tail current analysis. For voltage-clamp recordings the leakage and capacitive currents were subtracted by using a P/−4 protocol (four negative correction pulses, with amplitude one-fourth of that of the test pulse). In current-clamp recordings, bridge balance and capacitance compensation were performed. Access resistance was monitored continuously, and only cells with access resistance <20 MΩ were used.

Extracellular recordings. For extracellular recordings the slices were transferred to an interface chamber (32–34°C; Fine Science Tools, Vancouver, British Columbia). We recorded extracellular potentials with glass micropipettes filled with ACSF (1–3 MΩ). Recording electrodes were positioned in the CA1 pyramidal cell layer, and signals were acquired via an A-M Systems amplifier (low filter, 1.0 Hz; high filter, 5.0 kHz; 1000×) (model 1800 Microelectrode, A-M Systems, Sequim, WA). Before spontaneous field activity was recorded, slice viability and stability were verified by the recording of evoked field EPSPs. Glass micropipettes filled with ACSF were used to stimulate electrically the Schaffer collateral pathway (0.03 Hz). Stable recordings ($\sim$20 min) with a population spike that had peak-to-peak amplitudes of >10 mV were used.

Reagents. TTX, ω-conotoxin-GVIA, and ω-agatoxin IVA were purchased from Alamone Labs (Jerusalem, Israel); ω-conotoxin MVIIC from Bachem (Torrance, CA); nickel (II) chloride from J.T. Baker (Paris, KY); pirenzepine, protein phosphatase 2 (PP2), and 2-[1-(3-dimethylaminopropyl)indol-3-yl]-3-(indol-3-yl) maleimide (GF 109203x) from Tocris (Ellisville, MO); BAPTA from Molecular Probes (Eugene, OR); 3-[1-3-(amidinothio)-propyl-^1H-indol-3-yl]-3-(1-methyl-^1H-indol-3-yl)maleimide (Ro 31-8220), 2-[N-(2-hydroxyethyl)]-N-(4-methoxybenzenesulfonyl)amino-N-(4-chlorocinnamyl-N-methyl-benzylamine) (KN-93), and 12-(2-cyanoethyl)-6,7,12,13-tetrahydro-13-methyl-5-oxo-^5H-indolo(2,3-a)pyrrolo(3,4-c)-carbazole (Go 6976) from Calbiochem (La Jolla, CA); all other reagents were purchased from Sigma (St. Louis, MO).

Data analysis. Data were analyzed with Clampfit 9.0 (Molecular Devices). In all cases Student's t tests were used for statistical comparisons, with $p < 0.001$ considered significant. Values are reported as the mean $\pm$ SEM.

Results

Carbachol enhances toxin-resistant HVA R-type currents but does not affect low voltage-activated T-type Ca^{2+} currents

We tested the hypothesis that muscarinic receptor stimulation enhances R-type VSCCs in CA1 pyramidal neurons similar to the muscarinic enhancement of recombinant Ca$_V$2.3 VSCCs described in human embryonic kidney (HEK) 293 cells (Melliti et al., 2000; Bannister et al., 2004). We performed voltage-clamp recordings to characterize the cholinergic modulation of the toxin-resistant Ca^{2+} currents, which were isolated with a mixture containing TTX, nifedipine, and VSCC toxins (as described in Materials and Methods). CA1 pyramidal neurons from hippocampal slices were patch clamped with a Cs$^+$- and TEA$^+$-based intracellular solution to suppress K$^+$ channels and to minimize muscarinic-mediated effects on K$^+$ channels. The ACSF contained Cs$^+$ and 4-AP to block potassium current and to increase the space-clamp efficiency. Under these conditions we observed an enhancement of HVA Ca^{2+} currents. In the presence of the VSCC blocker mixture toxin-resistant low (T-type) and high (R-type) voltage-activated transient Ca^{2+} currents were recorded in all cells (Fig. 1A). The classification of currents was based on the potentials for activation, toxin resistance, and Ni^{2+} sensitivity. Only the HVA R-type current was enhanced dramatically after the application of carbachol ($n = 13$) (Fig. 1B). This carbachol-mediated stimulation was reversible ($n = 6$) (Fig. 1C), and the currents were sensitive to 50 μM Ni^{2+} ($n = 5$) (Fig. 1D). Strikingly, the I–V curve of the Ca^{2+} currents showed that the T-type component (observed as a shoulder in the I–V at −60 to −30 mV) was not affected, whereas the peak of the R-type current was enhanced dramatically in carbachol (Fig. 1E). The averaged I–V curve before and after carbachol treatment is shown in Figure 2A ($n = 7$). The peak amplitudes of T-type and R-type currents are plotted in Figure 2B, showing that the T-type component did not change (99.6 $\pm$ 2% of control; $p = 0.76$; $n = 10$), whereas the R-type component increased significantly (154 $\pm$ 4% of control; $p < 0.0001$; $n = 13$). The example traces for T-type and R-type are shown in Figure 2C. The enhanced amplitude of the R-type Ca^{2+} current was associated consistently with a significant shift of the voltage-dependent activation curve to negative potentials, with a change in the voltage for half-maximal activation (V_{act}) ($\Delta V_{act} = -4.2 \pm 0.7$ mV; $p < 0.001$; $n = 7$) (Fig. 2D). The enhancement of R-type Ca^{2+} currents was reversible and blocked by atropine (1 μM), demonstrating that it was attributable to muscarinic receptor activation by carbachol ($n = 6$) (Fig. 2E). Pooled data for
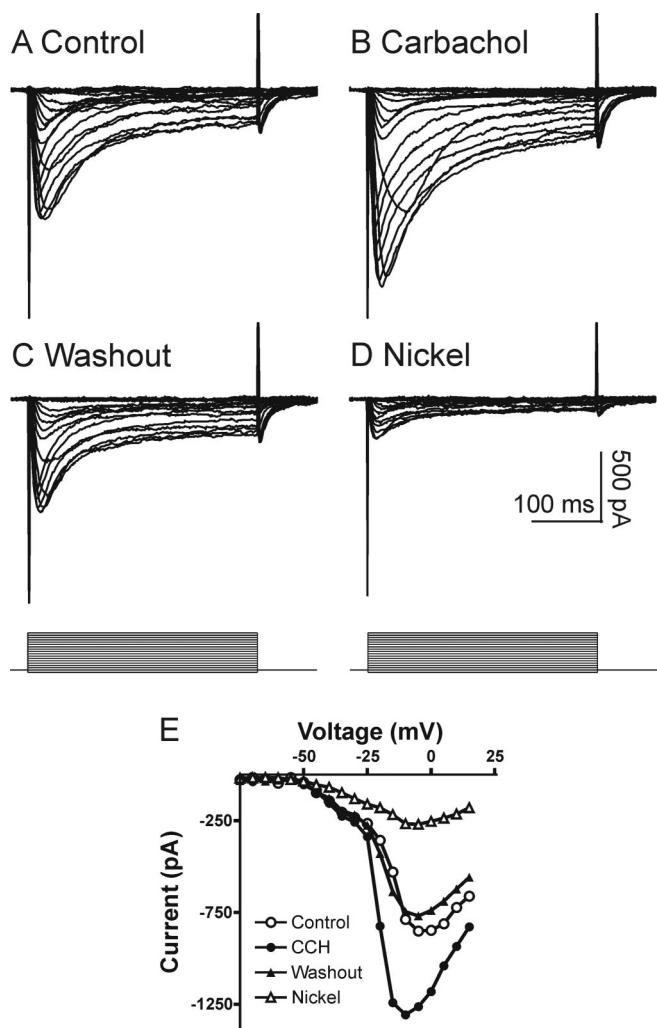
Figure 1. Carbachol enhances toxin-resistant HVA Ca^{2+} currents. Whole-cell patch-clamp recordings were performed with a Cs^+- and TEA^+-based intracellular solution. Slices were preincubated with toxins (as described in Materials and Methods) and perfused with TTX (1.2 μM) and nifedipine (20 μM). *A*, In voltage-clamp mode, a well clamped Ca^{2+} current was recorded. *B*, The current was enhanced by the application of carbachol (30 μM). This enhancement was reversible (*C*) and sensitive to Ni^{2+} (50 μM; *D*). *E*, *I–V* relationships of this cell before and after treatment, showing that the T-type component (observed as a shoulder at −60 to −30 mV in the *I–V*) was not affected, whereas the peak of the R-type current was enhanced dramatically in carbachol (CCH).
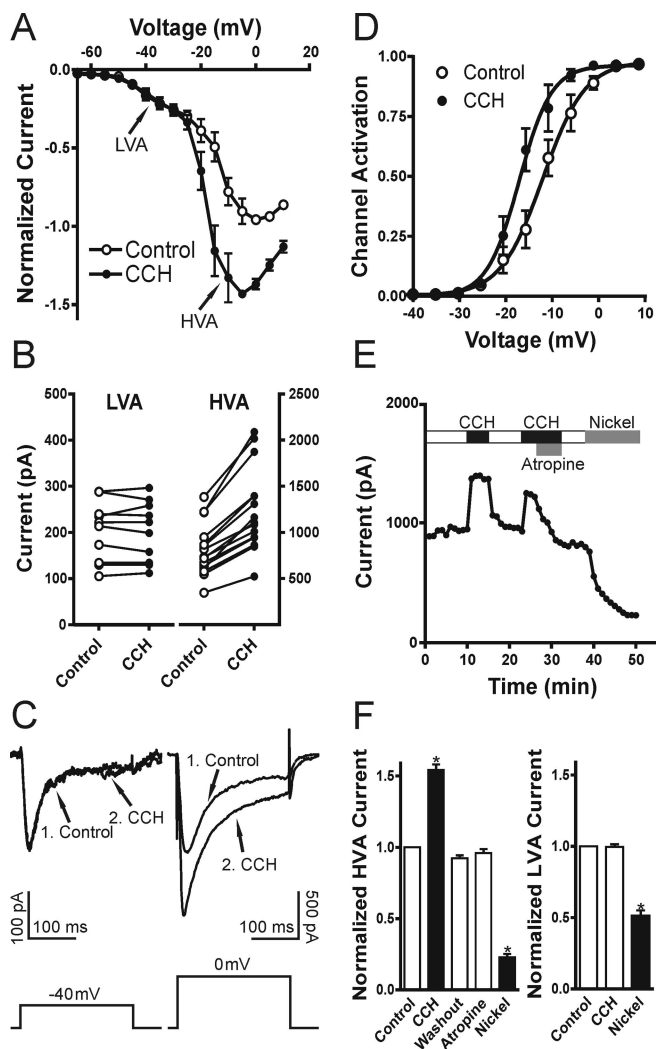

Figure 2. Muscarinic activation enhances R-type, but not T-type, Ca^{2+} current. *A–C*, HVA, but not LVA, component is stimulated by muscarinic activation. The mean *I–V* relationships before and after carbachol (CCH) treatment from seven cells are shown in *A*. The peak current amplitudes and sample traces are shown in *B*, *C* (1, Control; 2, CCH). *D*, The Ca^{2+} channel activation curve analyzed from peak currents and estimated conductance is shifted significantly to the left. The result was similar when tail currents were analyzed (data not shown). The result was fit with a Boltzmann equation. *E*, Time course of the peak HVA Ca^{2+} current shows that carbachol (CCH) stimulation of R-type VSCCs is reversible and is blocked by the muscarinic receptor antagonist atropine (1 μM). *F*, Mean data for the muscarinic modulation of the LVA and HVA Ca^{2+} current components. All recordings were obtained in TTX and VSCC blockers (as described in Materials and Methods). Error bars indicate the mean ± SEM. Asterisk indicates significant change (*$p < 0.001$).

muscarinic modulation of R-type and T-type VSCCs are shown in Figure 2*F* (for each group, $n \geq 5$). These results suggest that, in CA1 pyramidal neurons, muscarinic activation enhances only the HVA R-type Ca^{2+} currents, but not the low voltage-activated (LVA) T-type Ca^{2+} currents.

To verify additionally that T-type Ca^{2+} currents were not modulated by muscarinic activation, we first blocked all HVA Ca^{2+} currents by perfusing 30 μM Cd^{2+} instead of the strategy used above with toxins and nifedipine. This is effective for isolating T-type Ca^{2+} currents, because the HVA Ca^{2+} currents are much more sensitive to low concentrations of Cd^{2+} (Ozawa et al., 1989; Mogul and Fox, 1991; Avery and Johnston, 1996; Huguenard, 1996). Under these conditions a LVA component was observed with no apparent HVA component ($n = 7$) (Fig. 3*A*). Application of Cd^{2+} (30 μM) only slightly decreased T-type Ca^{2+} currents (91 ± 6% of control; $p = 0.68$; $n = 7$) (Fig. 3*B,C*), whereas the R-type Ca^{2+} currents were abolished (11 ± 7% of

control; $p < 0.0001$; $n = 7$) (Fig. 3*B,D*). We then tested the modulation of Cd^{2+}-isolated T-type Ca^{2+} currents by muscarinic receptor activation. In agreement with our results described above, we did not observe any significant alteration of the isolated T-type Ca^{2+} currents by carbachol (104 ± 7% of control; $p = 0.57$; $n = 6$) (Fig. 3*E–G*). The averaged *I–V* curves for the effects of carbachol on T-type Ca^{2+} currents are shown in Figure 3*F*. Application of Ni^{2+} (50 μM) suppressed this current by ~50% ($n = 5$; $p < 0.0001$) (Fig. 3*E,G*). Because low micromolar concentrations of Ni^{2+} block only α1H subunits, but not α1G or α1I (Klockner et al., 1999; Lee et al., 1999; Perez-Reyes, 2003), our results suggest the existence of multiple subunits of T-type VSCCs in CA1 pyramidal neurons, which is consistent with previous *in situ* hybridization work (Talley et al., 1999). These results
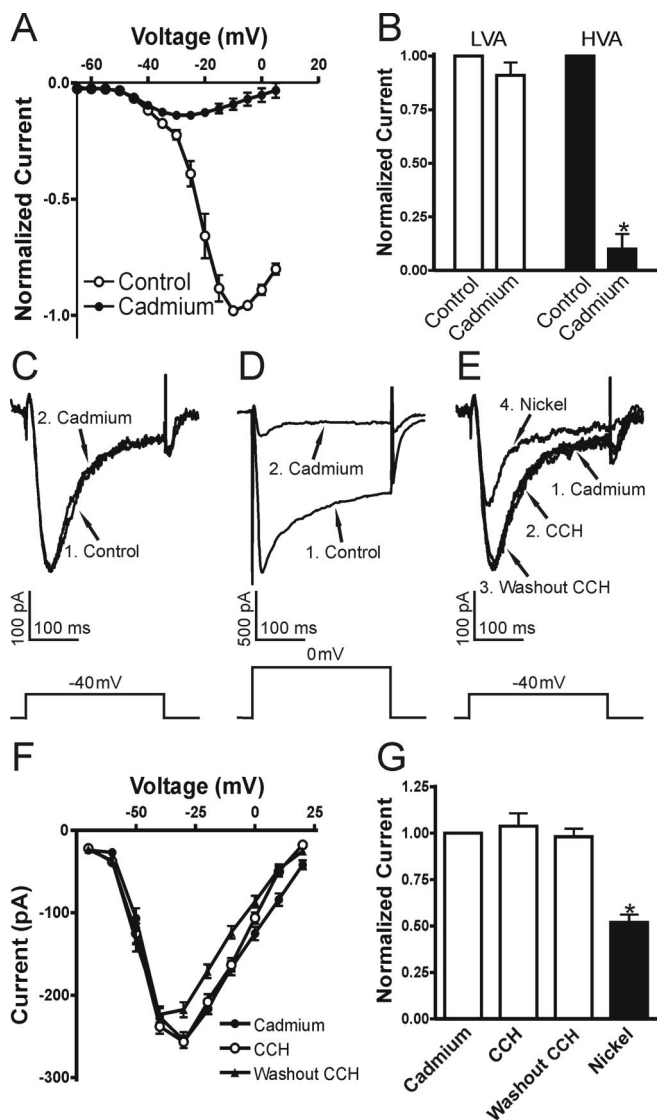
Figure 3. T-type Ca^{2+} current is not affected in carbachol. Cd^{2+} (30 μM) was used to isolate the LVA VSCCs. **A**, Mean *I–V* curve of Cd^{2+}-isolated Ca^{2+} current (*n* = 7). Mean data for Cd^{2+} effects in **B** show that the LVA component was decreased slightly, whereas the HVA component was nearly diminished by Cd^{2+} (30 μM). **C, D**, Sample traces for LVA and HVA currents before (1, Control) and after (2, Cadmium) Cd^{2+} treatment are shown. **E**, The Cd^{2+}-isolated LVA Ca^{2+} current (1, Cadmium) was not affected by carbachol (2, CCH) or during washout (3, Washout CCH) but was blocked partially by subsequent treatment with Ni^{2+} (4, Nickel; 50 μM). **F**, Mean *I–V* curves for effects of carbachol (CCH and Washout CCH) on the Cd^{2+}-isolated T-type Ca^{2+} currents (*n* = 5). **G**, Mean data for muscarinic modulation of Cd^{2+}-isolated T-type VSCCs (for each group, *n* ≥ 5). Error bars indicate the mean ± SEM. Asterisk indicates significant change (*p < 0.001).

Figure 4. M_1/M_3 muscarinic subtypes mediate the stimulation of R-type Ca^{2+} current. **A–C**, The M_1 antagonist pirenzepine (1 μM) reversed the stimulation of R-type VSCCs by carbachol (CCH). *I–V* curves and sample traces are shown in **A, B** (1, Control; 2, CCH; 3, Pirenzepine). **C**, Mean data for the effects of pirenzepine (1 μM), 4-DAMP (1 μM; M_1/M_3 antagonist), and methoctramine plus tropicamide (1 μM; M_2 and M_4 antagonists) on the enhancement of R-type VSCCs. **D–F**, M_1 agonist McN-A-343 (100 μM) mimicked and occluded the stimulation of R-type VSCCs by carbachol (CCH). *I–V* curves and sample traces are shown in **D, E** (1, Control; 2, McN-A-343; 3, CCH). **F**, Mean data for the effects of McN-A-343 and the subsequent application of carbachol (CCH) on R-type VSCCs. All recordings were obtained in TTX and VSCC blockers (as described in Materials and Methods). Error bars indicate the mean ± SEM. Asterisk indicates significant change (*p < 0.001).

confirmed that, in CA1 pyramidal neurons, muscarinic activation had no effect on T-type Ca^{2+} currents.

M_1/M_3 cholinergic receptors mediate muscarinic stimulation of R-type VSCCs

The ability of atropine (1 μM) to block the stimulation of carbachol in R-type Ca^{2+} currents demonstrates that muscarinic receptors mediate this enhancement. In the hippocampus four of the muscarinic subtypes (M_1–M_4) are expressed abundantly (Vilaro et al., 1993; Levey et al., 1995; Rouse et al., 1999). To determine further the muscarinic receptor subtypes involved in the enhancement of R-type Ca^{2+} currents, we tested the antagonists and agonists for M_1–M_4 cholinergic receptors. We found
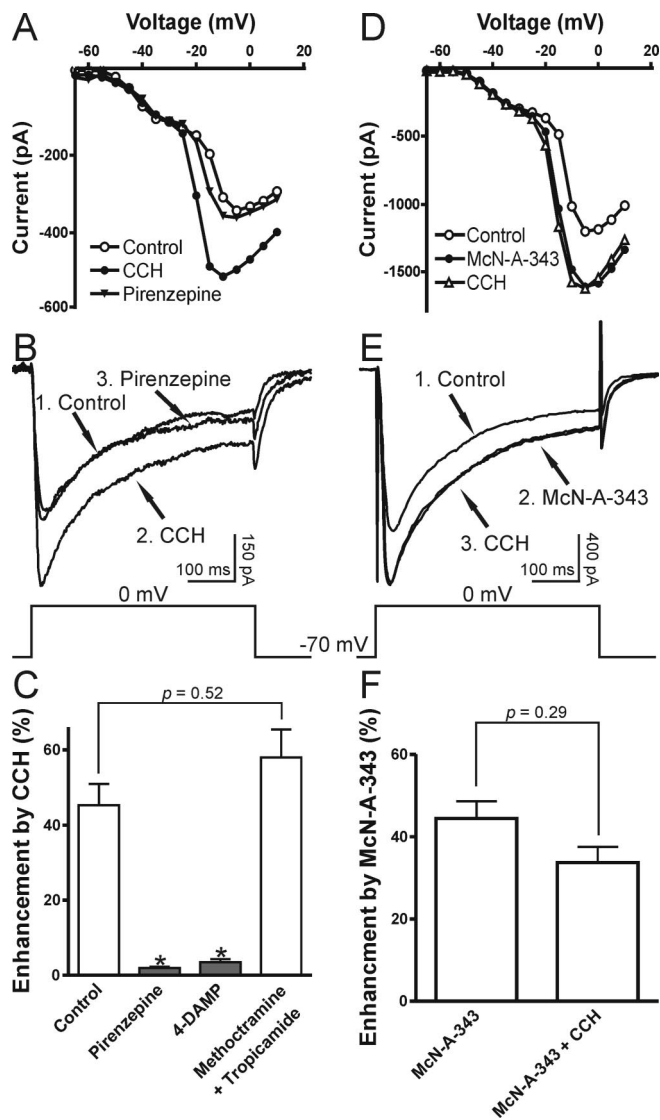
that both pirenzepine (1 μM; *n* = 5), a M_1-specific antagonist, and 4-diphenylactoxy-*N*-methylpiperidine (4-DAMP; 1 μM; *n* = 4), an antagonist with equal affinity to both M_1 and M_3 receptors, could reverse the carbachol enhancement of R-type Ca^{2+} currents (Fig. 4*A–C*). In contrast, the M_2/M_4 antagonists methatropine (1 μM) and tropicamide (1 μM) had no effect (*n* = 5) (Fig. 4*C*). To confirm the involvement of M_1/M_3 subtypes, we tested the M_1 agonist 4-*N*-[3-chlorophenyl]carbamoyloxy-2-butynyl-trimethylammonium chloride (McN-A-343; 100 μM). We found that McN-A-343 mimicked the carbachol-mediated enhancement of R-type Ca^{2+} currents (*n* = 6), and, when applied first, McN-A-343 occluded additional enhancement by the subsequent treatment of carbachol (30 μM; *n* = 4) (Fig. 4*D–F*). Thus

the muscarinic enhancement of R-type Ca^{2+} currents is mediated by M_1/M_3 subtypes.

Muscarinic modulation of R-type VSCCs requires a Ca^{2+}-independent PKC pathway

In recombinant systems the stimulation of $Ca_V2.3$ Ca^{2+} currents is dependent on phosphorylation that is mediated by a pathway coupled to a pertussis toxin-insensitive $G\alpha$ subunit ($G\alpha_{q/11}$) (Bannister et al., 2004). M_1/M_3 receptors couple to $G\alpha_q$ subunits to stimulate phospholipase $C\beta_1$ ($PLC\beta_1$), which initiates phosphatidylinositol 4,5-bisphosphate (PIP_2) turnover. This leads to the production of diacylglycerol (DAG) and IP_3-mediated Ca^{2+} release, which in turn activates protein kinase C (PKC). Basically, there are three groups of PKCs: the Ca^{2+}- and DAG-dependent isoforms (group I), the Ca^{2+}-independent but DAG-dependent isoforms (group II), and the atypical isoforms (group III). We examined the signaling mechanisms underlying the enhancement of R-type Ca^{2+} currents by first testing the Ca^{2+} dependence and then by examining the sensitivity to different PKC inhibitors. A high concentration of high-affinity Ca^{2+} chelator BAPTA (10 mM) was used in the pipette solution, which has proved to be sufficient to block completely the carbachol-induced plateau potentials or tail currents in our lab (Fraser and MacVicar, 1996; Kuzmiski and MacVicar, 2001). We found that 10 mm BAPTA could not prevent the carbachol enhancement of R-type VSCCs ($n = 5$) (Fig. 5 A,D), suggesting it involves a Ca^{2+}-independent pathway. To investigate the potential involvement of PKC in the enhancement of R-type VSCCs, we preincubated slices for >30 min with the broad spectrum PKC antagonists GF 109203x (10 μM; $n = 5$) or Ro 31-8220 (10 μM; $n = 5$). In the presence of these PKC antagonists carbachol did not enhance R-type Ca^{2+} currents (Fig. 5 B,E), suggesting that PKCs are involved in this modulation. Interestingly, in the presence of PKC inhibitors (GF 109203x or Ro 8332) a significant suppression of R-type Ca^{2+} currents was observed by muscarinic stimulation (Fig. 5 B,E). This inhibitory effect probably results from the activation of pertussis toxin-sensitive G-protein-coupled M_2/M_4 receptors and $G\beta\gamma$ subunit-mediated inhibition (Meza et al., 1999; Bannister et al., 2004). Because we observed a stable enhancement of R-type currents in normal conditions, we did not study this inhibitory effect further. To determine which group of PKCs is involved, we applied the specific group I (Ca^{2+}-dependent) PKC inhibitor Go 6976 (10 μM; $n = 5$). Application of Go 6976 did not block the carbachol-mediated enhancement of R-type Ca^{2+} currents (Fig. 5 C,E). Ca^{2+}/calmodulin-dependent protein kinase II (CaMKII) and Src-family signaling pathways also have been reported to be involved in some muscarinic-activated pathways. However, we found that inhibitors of CaMKII (KN-93, 10 μM; $n = 6$) and Src-kinase (PP2, 10 μM; $n = 5$) had no effect on the muscarinic stimulation of R-type Ca^{2+} currents at concentrations that have been reported to be effective in brain slices (Fig. 5E) (Zhao et al., 2004; Grishin et al., 2005; Huang et al., 2005). This pattern of sensitivity to PKC antagonists and insensitivity to BAPTA suggests the involvement of Ca^{2+}-independent PKCs in the muscarinic effect on R-type Ca^{2+} currents.

Muscarinic enhancement of R-type Ca^{2+} spikes

Current-clamp recordings also were performed to characterize the cholinergic modulation of the toxin-resistant Ca^{2+} spikes. CA1 pyramidal neurons from hippocampal slices also were patch-clamped with a Cs^+-based intracellular solution to suppress K^+ channels and to minimize muscarinic-mediated effects on K^+ channels. When recordings were obtained from CA1 neu-
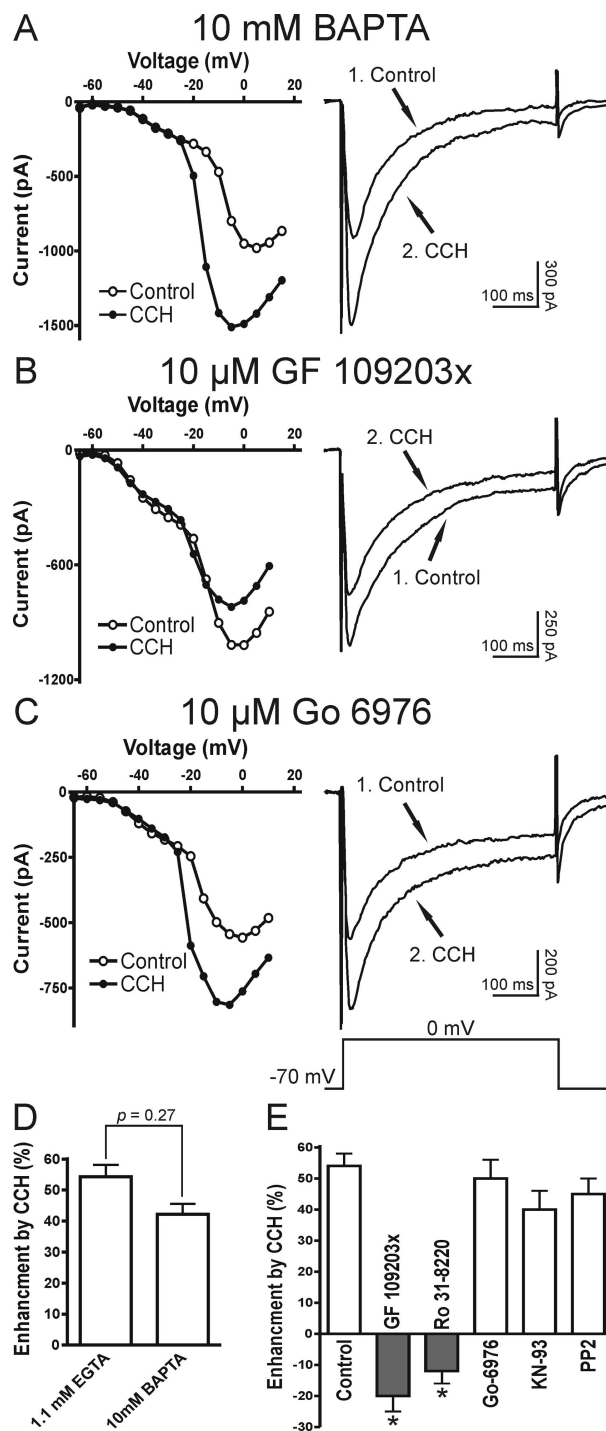

Figure 5. Mechanisms underlying the muscarinic stimulation of R-type VSCCs. **A**, Ca^{2+} independence of muscarinic enhancement of R-type VSCCs. In a CA1 pyramidal neuron recorded with 10 mM BAPTA-based intracellular solution, the R-type Ca^{2+} current is enhanced in carbachol (1, Control; 2, CCH). **B, C**, A Ca^{2+}-independent PKC pathway is involved in the muscarinic modulation of R-type VSCCs (1, Control; 2, CCH). **B**, Preincubation of the broad spectrum PKC blocker GF 109203x (10 μM) abolishes the muscarinic stimulation of R-type Ca^{2+} currents and, conversely, results in current depression. **C**, After preincubation of the group I PKC (Ca^{2+}-dependent isoforms) inhibitor Go 6976 (10 μM), the muscarinic stimulation of R-type VSCCs is not affected. **D**, Mean data for the effects of intracellular solutions containing either 1.1 mM EGTA or 10 mm BAPTA on the muscarinic enhancement of R-type VSCCs. **E**, Mean data for the effects of GF 109203x (10 μM), Ro 31-8220 (10 μM; broad spectrum PKC blocker), Go 6976 (10 μM), KN-93 (10 μM; CaMKII blocker), and PP2 (10 μM; Src tyrosine kinase inhibitor) on the muscarinic modulation of R-type VSCCs (for each group, $n \geq 5$). All recordings were obtained in TTX and VSCC blockers (as described in Materials and Methods). Error bars indicate the mean ± SEM. Asterisk indicates significant change (*$p < 0.001$).

rons in TTX without a blocking of any Ca^{2+} currents, large-amplitude prolonged plateau Ca^{2+} spikes were evoked by injection of brief (40 ms) intracellular current pulses ($n = 7$) (Fig. 6A,B). Carbachol depressed the plateau Ca^{2+} spikes, consistent with a muscarinic depression of L-, N-, and P/Q-type VSCCs, leaving only a transient HVA Ca^{2+} spike. A significant portion of this calcium spike in carbachol could be attributable to R-type Ca^{2+} currents, because it was Ni^{2+}-sensitive ($n = 4$). These results suggest that muscarinic receptor activation in hippocampal neurons could shift the normal pattern of Ca^{2+} entry from the slowly inactivating N-, P/Q-, and L-type VSCCs to domination by the HVA rapidly inactivating R-type VSCCs.

To delineate rigorously the direct action of carbachol on the toxin-resistant Ca^{2+} spikes, we isolated them with a mixture containing TTX, nifedipine, and toxins, as shown in previous voltage-clamp experiments. Under these conditions depolarization of neurons with intracellular current injection often led to the generation of a transient HVA Ca^{2+} spike ($n = 50$ of 69). The Ca^{2+} spike inactivated during the depolarizing command pulses, consistent with a Ca^{2+} spike mediated by rapidly inactivating HVA R-type Ca^{2+} currents (Randall and Tsien, 1997). However, even with strong current injection (≥ 0.5 nA) numerous cells (28%; $n = 19$ of 69) remained silent. As shown previously with current-clamp recordings (Kuzmiski et al., 2005), subsequent bath application of carbachol resulted in persistent enhancement of R-type Ca^{2+} spiking in both the spiking and initially silent neurons (Fig. 6C,D). The initially silent neurons exhibited transient Ca^{2+} spikes in the presence of carbachol ($n = 19$) (Fig. 6C,D). In neurons that initially showed an R-type Ca^{2+} spike, carbachol induced an increase in spike amplitude ($\Delta AP_{AMP} = 5.7 \pm 0.7$ mV; $p < 0.0001$; $n = 50$), a decrease in the threshold for spike activation ($\Delta AP_{TH} = -6.7 \pm 0.8$ mV; $p < 0.0001$; $n = 50$), and a reduction in the current injection required to evoke a spike ($\Delta I = -80 \pm 12$ pA; $p < 0.0001$; $n = 50$) (Fig. 6F). These enhanced spikes were blocked by the application of Ni^{2+} (50 μM; $n = 20$) (Fig. 6E,G,H), which at this concentration is selective for R- and T-type VSCCs. This enhancement was not caused by a muscarinic-mediated increase in input resistance (R_{IN}) (control R_{IN}, 115.7 $\pm$ 5.9 MΩ vs carbachol R_{IN}, 118.0 $\pm$ 6.1 MΩ; $p = 0.77$; $n = 69$). The application of high concentrations of nimodipine (20 μM) sufficient to block partially the T-type VSCCs had no effect on the carbachol-enhanced HVA Ca^{2+} spikes (percentage of ΔAP_{AMP}, 3.5 $\pm$ 2.6%; $p = 0.25$; percentage of $\Delta dV_m/dt_{max}$, $-5.2 \pm 9.1\%$; $p = 0.38$; $n = 5$) (Fig. 6G,H). In addition, the Ca^{2+} spikes were only weakly voltage dependent when held at depolarized voltages (from -70 to -60 mV) (percentage of ΔAP_{AMP},
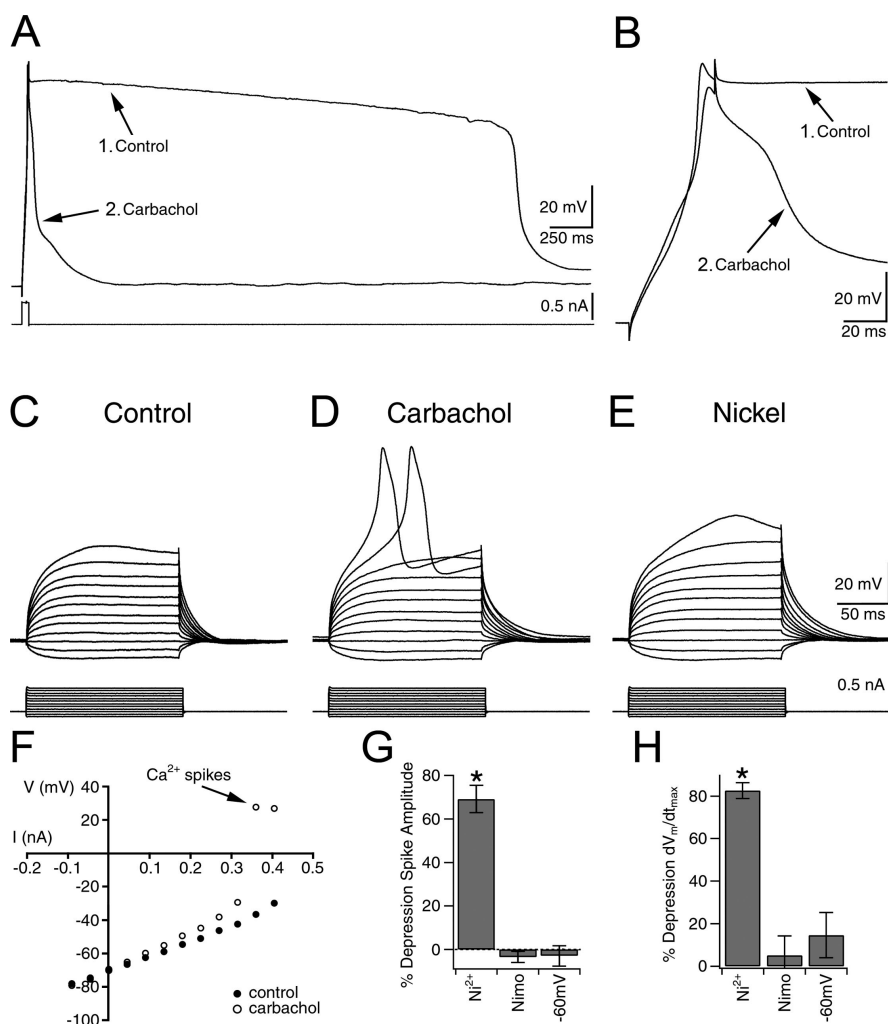

Figure 6. R-type VSCC-dependent spikes are enhanced by carbachol. **A**, Ca^{2+} spikes evoked by current injection before (1, Control) and after (2) carbachol application. **B**, Expanded view of Ca^{2+} spikes in **A** before (1, Control) and after (2) carbachol in TTX, but with no VSCC blockers. In carbachol, a HVA Ca^{2+} spike remains. **C**, Silent neuron in the presence of 1.2 μM TTX, 20 μM nifedipine, ω-conotoxin MVIIC, ω-conotoxin-GVIA, and ω-agatoxin IVA, as described in the voltage-clamp experiments. **D**, Activation of R-type VSCC-dependent spikes is observed only after the application of carbachol. **E**, Application of 50 μM Ni^{2+} (R-type VSCC blocker) depresses carbachol-enhanced R-type Ca^{2+} spikes. **F**, Plot of I–V relationship before and after carbachol. Note the activation of R-type Ca^{2+} spikes in carbachol. **G, H**, Effects of 50 μM Ni^{2+} ($n = 20$), 20 μM nimodipine (Nimo; L- and T-type VSCC blocker; $n = 5$), and membrane depolarization to -60 mV ($n = 5$) on the peak amplitude or the maximum rate of rise (dV_m/dt_{max}) of the carbachol-enhanced R-type Ca^{2+} spikes as compared with spikes evoked in carbachol. Error bars indicate the mean $\pm$ SEM. Asterisk indicates significant depression (*$p < 0.001$).

2.9 $\pm$ 4.8%; $p = 0.82$; percentage of $\Delta dV_m/dt_{max}$, $-14.6 \pm 10.6\%$; $p = 0.24$; $n = 5$) (Fig. 6G,H). Consistent with our voltage-clamp results, we concluded that R-type, but not T-type, Ca^{2+} currents generated the toxin-resistant Ca^{2+} spikes.

Muscarinic enhancement of R-type Ca^{2+} spikes contributes to carbachol-induced theta burst oscillations

The cholinergic system is implicated in the generation of theta both *in vitro* and *in vivo* (Buzsaki, 2002). During theta *in vivo* the HVA Ca^{2+} spikes oscillate rhythmically at theta frequencies in the dendrites of CA1 pyramidal neurons and may contribute to current generation and amplification of theta (Kamondi et al., 1998; Buzsaki, 2002). However, the VSCC subtypes that contribute to dendritic oscillations during theta are unknown. We examined the possibility that muscarinic-enhanced R-type Ca^{2+} spikes can resonate at theta frequency and thereby contribute to the generation of dendritic oscillations. To evaluate the firing
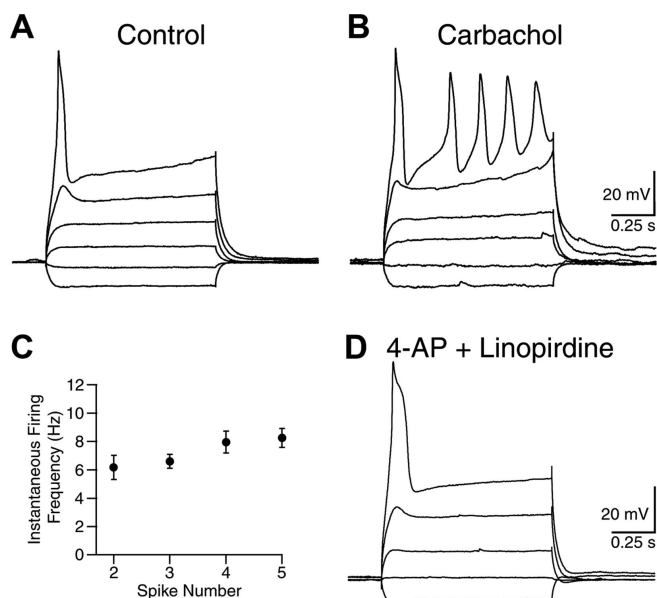
A Control   **B** Carbachol

20 mV
0.25 s

C   **D** 4-AP + Linopirdine

20 mV
0.25 s

Figure 7. Muscarinic-enhanced R-type Ca^{2+} spikes fire repetitively at theta frequency. **A**, R-type Ca^{2+} spike evoked by injection of a long (1.0 s) depolarizing current pulse. **B**, Repetitive R-type Ca^{2+} spiking evoked during a long current pulse after the application of carbachol. **C**, Instantaneous firing frequency of repetitive R-type Ca^{2+} spikes after carbachol treatment ($n = 11$). Error bars indicate the mean $\pm$ SEM. **D**, Application of 5 mM 4-AP (K$^+$ channel blocker) and 10 μM linopirdine (M-current blocker) failed to induce the repetitive R-type Ca^{2+} spiking ($n = 3$).

frequencies of R-type Ca^{2+} spikes, we injected long (0.5–1.0 s) depolarizing steps of current in neurons in the presence of TTX, VSCC toxins, and nifedipine as described above. Under these conditions either the cells were silent or only a single spike could be evoked even with strong current injection (Fig. 7A). After the addition of carbachol to the perfusate, R-type Ca^{2+} spiking was enhanced, and now multiple spikes could be evoked (Fig. 7B). Interestingly, repetitive R-type Ca^{2+} spiking displayed a regular rhythm in the theta frequency range (6–9 Hz; $n = 11$) (Fig. 7C). Application of K$^+$ channel blockers (4-AP, 5 mM; linopirdine, 10 μM) failed to mimic this repetitive firing pattern ($n = 3$) (Fig. 7D), suggesting that the ability of the R-type Ca^{2+} spikes to fire at theta frequency is attributable to direct actions on R-type VSCCs. To avoid the generation of plateau potentials (Fraser and MacVicar, 1996), we limited our recordings to <1 s. These findings indicate that carbachol-enhanced R-type Ca^{2+} spiking could contribute to the intrinsic resonant depolarizations of CA1 pyramidal neurons in the theta frequency.

To examine the potential contribution of muscarinic-enhanced R-type VSCCs to theta burst oscillatory activity, we also recorded spontaneous extracellular events from area CA1. In the majority of naive hippocampal slices the theta frequency oscillations were generated after continuous bath application of carbachol (Fig. 8A). Field potential recordings showed a peak power spectra of 0.016 $\pm$ 0.0071 mV^2/Hz at a mean frequency of 8.3 $\pm$ 0.6 Hz ($n = 8$) (Fig. 8B). The spontaneous oscillatory bursts occurred at regular intervals of 101.4 $\pm$ 10.9 s ($n = 8$) and lasted for 21.4 $\pm$ 2.6 s. Theta burst oscillations closely resembled those previously described (Bland et al., 1988). Subsequent application of a low concentration of Ni^{2+} depressed the oscillatory activity, as shown by an almost complete abolition of the power in the theta frequency range ($n = 8$ of 8) (Fig. 8A,B). In five of eight slices the oscillatory bursts were abolished completely. In the other three slices Ni^{2+} reduced the amplitude of the theta burst oscillations and increased the interburst interval without signifi-

cant effects on burst durations (19.3 $\pm$ 2.8 s; $n = 3$) or the frequency of the oscillations (8.3 $\pm$ 0.4 Hz). Disruption of the theta bursts often was accompanied by a change in the field events to a slower, more interictal-like pattern. Because we demonstrated that T-type VSCCs are not affected by cholinergic stimulation, these results suggest that Ni^{2+} suppressed the carbachol-induced spontaneous field potential theta oscillations by depressing R-type VSCCs. Therefore, our results indicate that in CA1 pyramidal neurons the enhancement of R-type VSCCs could contribute to muscarinic-induced theta frequency oscillations.

Discussion

Our results show that muscarinic activation stimulates R-type Ca^{2+} currents in hippocampal CA1 neurons that can lead to *de novo* activation of R-type dependent Ca^{2+} spikes. This enhancement likely is mediated via a Ca^{2+}-independent PKC pathway because it is blocked by broad spectrum inhibitors to PKC, but not by an inhibitor of Ca^{2+}-dependent PKC, and it is insensitive to chelation of intracellular Ca^{2+} by BAPTA. In contrast to the enhancement of the R-type currents, T-type Ca^{2+} currents were not modulated by muscarinic receptor activation. The muscarinic-mediated enhancement of transient R-type Ca^{2+} spikes resulted in remarkable changes in the firing pattern of R-type Ca^{2+} spikes and could contribute to theta oscillations.

Mechanisms underlying muscarinic enhancement of R-type VSCCs

R-type Ca^{2+} currents in hippocampal neurons are attributable mainly to Ca$_V$2.3 subunits (Sochivko et al., 2002, 2003), although there is still some controversy as to the proportion of R-type Ca^{2+} currents that remains in the Ca$_V$2.3 knock-out mouse (Wilson et al., 2000). In recombinant systems Ca$_V$2.3 subunit Ca^{2+} currents are enhanced by G$\alpha_{q/11}$-coupled muscarinic receptor activation (Bannister et al., 2004; Kamatchi et al., 2004). Here we show a similar enhancement of R-type Ca^{2+} currents in hippocampal neurons also mediated by muscarinic M$_1$/M$_3$ receptor stimulation. Hippocampal pyramidal neurons express high levels of postsynaptic M$_1$ and M$_3$ receptors (Vilaro et al., 1993; Levey et al., 1995; Rouse et al., 1999). These receptors are G$\alpha_{q/11}$ coupled, and their activation results in the generation of DAG and IP$_3$ via PLC activation. DAG and IP$_3$ in turn activate PKC and IP$_3$ receptor pathways, respectively. Similar to previous work in HEK cells and *Xenopus* oocytes (Bannister et al., 2004; Kamatchi et al., 2004), the muscarinic stimulation of R-type VSCCs in hippocampal neurons was independent of intracellular Ca^{2+} and required the activation of Ca^{2+}-independent group II PKCs. All three groups of PKCs are expressed in rat hippocampus (Naik et al., 2000), and PKCδ from among the group II PKCs (δ, ε, η, and θ) may be the isoform of PKC that is involved. PKCδ is highly expressed in rat hippocampal CA1 pyramidal neurons (McNamara et al., 1999; Tang et al., 2004), and in response to muscarinic stimulation PKCδ is activated and translocated to plasma membrane (Brown et al., 2005). In recombinant systems the co-expression of a dominant-negative PKCδ blocked the muscarinic stimulation of Ca$_V$2.3 subunits, whereas the blocker of PKCε could not (Bannister et al., 2004). However, we could not rule out definitively the contribution of other isoforms. In PKC inhibitors we observed a suppression of R-type Ca^{2+} currents by muscarinic stimulation, suggesting other inhibitory pathways. This inhibition may result from the activation of pertussis toxin-sensitive G-protein-coupled M$_2$/M$_4$ receptors and G$\beta\gamma$ subunit-mediated inhibition (Meza et al., 1999; Bannister et al., 2004).

R-type versus other VSCC types

Muscarinic enhancement of R-type VSCCs is strikingly opposite to muscarinic depression of all other HVA VSCCs (N-type, P-/Q-type, and L-type) (Gahwiler and Brown, 1987; Shapiro et al., 1999, 2001; Stewart et al., 1999). Christie and colleagues (1995) showed that in the soma and basal dendrites ($\leq 50\ \mu m$) all of the HVA VSCCs as well as LVA VSCCs contribute to spike-triggered Ca^{2+} entry. In contrast, T-type and Ni^{2+}-sensitive R-type VSCCs predominantly underlie spike-triggered Ca^{2+} entry in apical dendrites ($\geq 100\ \mu m$) (Christie et al., 1995). Single channel analysis also shows that all VSCC types are expressed in the soma, whereas in dendrites T- and R-type VSCCs predominate (Magee and Johnston, 1995). Action potential or depolarization-induced Ca^{2+} influx in dendrites and spines also has been shown to be mediated mainly by R-type VSCCs (Sabatini and Svoboda, 2000; Yasuda et al., 2003). The distinct distribution in apical dendrites and the unique modulation of R-type VSCCs suggest that they play a different role and underlie distinct cellular functions from other types of VSCCs, such as synaptic integration and plasticity.

Despite the general suppression of Ca^{2+} currents, muscarinic activation paradoxically increases intracellular Ca^{2+} accumulations in the dendrites and spines from depolarization or synaptic stimulation (Muller and Connor, 1991, 1992; Tsubokawa and Ross, 1997; Beier and Barish, 2000). K^+ conductance blockade and the IP_3-mediated release of Ca^{2+} from intracellular stores are thought to contribute to this accumulation (Muller and Connor, 1991, 1992; Tsubokawa and Ross, 1997; Beier and Barish, 2000). However, our results suggest that the stimulation of R-type Ca^{2+} currents also might contribute to the muscarinic-mediated intracellular Ca^{2+} accumulations.

All three T-type VSCC subunits ($\alpha 1G$, $\alpha 1H$, and $\alpha 1I$) are expressed in hippocampal pyramidal neurons (Talley et al., 1999). However, their modulation and functional impact on hippocampal pyramidal neurons are not yet known. Compared with HVA channels, T-type VSCCs are more metabolically stable and are less likely to be modulated (Huang et al., 2005). Muscarinic activation has been reported to increase, decrease, or not affect the T-type Ca^{2+} currents, depending on the cell type and experimental conditions (Yunker, 2003). In the present study T-type Ca^{2+} currents in hippocampal pyramidal neurons were not affected by muscarinic stimulation.

Muscarinic stimulation is known to suppress K^+ channels, such as M channels (Brown and Adams, 1980; Halliwell and Adams, 1982), thereby enhancing neuronal excitability. However, in the present study the enhancement of R-type Ca^{2+} currents is not attributable to K^+ channel depression. High concentrations of potassium channel blockers were applied both intracellularly and extracellularly (see Materials and Methods), and most K^+ currents were observed to be blocked. When the HVA Ca^{2+} currents were blocked first with Cd^{2+} (1 mM), muscarinic activation did not affect the residue K^+ currents (data not shown). In addition,
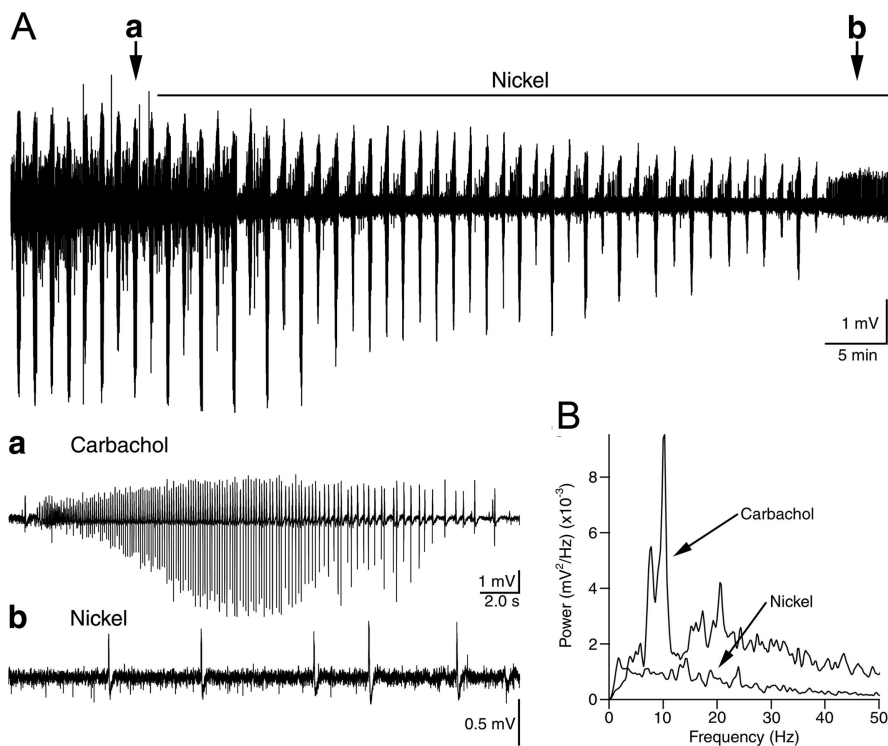

Figure 8. Carbachol-induced theta burst oscillations observed with extracellular recordings of field potentials are Ni^{2+} sensitive. ***A***, Extracellular recordings in area CA1 of spontaneous oscillatory bursts induced by perfusion with 40 μM carbachol before and after the application of 100 μM Ni^{2+}. The solid horizontal bar indicates the application of Ni^{2+}. ***a***, Expanded trace from ***A***, showing a spontaneous burst activated in carbachol. The arrow in ***A***, labeled a, indicates the location of the burst. ***b***, Expanded trace of the field potential recording after the application of Ni^{2+} indicated by the arrow in ***A***, labeled b. ***B***, Mean power spectra of the field potential oscillations in carbachol showing that the peak at theta frequency is abolished by Ni^{2+} ($n = 8$).

the repetitive R-type Ca^{2+} spike firing we observed in carbachol was not elicited with K^+ channel inhibitors. Furthermore, T-type Ca^{2+} currents were found to be unaltered by carbachol application. Under normal physiological conditions it is likely that the suppression of K^+ channels and enhancement of R-type VSCCs both contribute to the muscarinic stimulation of neuronal excitability.

A concern for this type of study is the possibility of poor voltage control during voltage-clamp experiments. To achieve well clamped currents, we applied high concentrations of K^+ channel blockers both intracellularly and extracellularly (Colino and Halliwell, 1993), and we used younger animals (13–16 d) so that the calcium currents would be smaller and the dendritic processes less extensive. Also, large electrode tips were used (3–5 MΩ), and only cells with access resistances <20 MΩ were included in the study. The voltage clamp appeared to be sufficient in most experiments because there was a graded turn-on of the currents, and channel activation properties of the currents were similar to those observed in acutely isolated neurons (Foehring et al., 2000; Sochivko et al., 2003).

R-type spikes and theta oscillations

Muscarinic receptor stimulation in the hippocampus *in vitro* generates robust oscillations, which share a common frequency with theta rhythm observed *in vivo*. The activation of oscillatory intrinsic conductances contributes importantly to theta current generation (Buzsaki, 2002). Voltage-dependent oscillations have been described in the somata (Leung and Yim, 1991) and dendrites of pyramidal neurons (Kamondi et al., 1998). During theta induction the somatic membrane hyperpolarizes, whereas den-

drites depolarize. When the dendritic depolarization is sufficiently strong, the resonant property of the membrane leads to a HVA Ca^{2+} spike-dependent self-sustained oscillation in the theta frequency range (Kamondi et al., 1998). Nickel ions selectively abolish dendritic calcium spikes via blocking R- and/or T-type VSCCs (Gillies et al., 2002; Isomura et al., 2002). Here we have demonstrated that carbachol-enhanced, Ni^{2+}-sensitive R-type Ca^{2+} spikes can fire repetitively at theta frequencies. Given that T-type VSCCs are not affected by carbachol, our results suggest that R-type VSCCs contribute to the amplification of the theta oscillations.

Based on pharmacological sensitivity, two types of theta could be distinguished: atropine-sensitive and atropine-resistant (Kramis et al., 1975; Buzsaki, 2002). Our results show that Ni^{2+} blocked carbachol-induced spontaneous theta burst oscillations. This agrees with a previous study demonstrating that Ni^{2+} (100 μM) blocked mGluR-activated but atropine-resistant theta oscillations (Gillies et al., 2002). In this previous study Ni^{2+}-dependent spikes were generated in the distal dendrites at theta frequencies. We found that the mGluR agonists *trans*-ACPD (*trans*-1-aminocyclopentane-1,3-dicarboxylic acid; 50 μM) and DHPG (dihydrophenylglycol; 50 μM) resulted in enhanced R-type Ca^{2+} spiking similar to that observed with carbachol (data not shown) (Kuzmiski and MacVicar, 2003). These results suggested that a similar contribution of R-type VSCCs to both atropine-sensitive and atropine-resistant forms of theta might exist.

In the hippocampus Ca^{2+} spikes are generated during highly synchronous excitatory input that is associated with behavior *in vivo*. The ability of carbachol-enhanced R-type Ca^{2+} spikes to resonate at theta frequencies suggests that it is an intrinsic property of the neuronal membrane that plays a key role in the generation of neuronal network oscillations. The resonance property of R-type VSCCs also may be important for synaptic plasticity induced by theta burst stimulation (Ito et al., 1995), the enhanced induction of theta during cholinergic stimulation (Huerta and Lisman, 1993), and the formation of accurate spatial memory (Kubota et al., 2001).

References

Avery RB, Johnston D (1996) Multiple channel types contribute to the low-voltage-activated calcium current in hippocampal CA3 pyramidal neurons. J Neurosci 16:5567–5582.

Bannister RA, Melliti K, Adams BA (2004) Differential modulation of $Ca_V2.3$ Ca^{2+} channels by Gαq/11-coupled muscarinic receptors. Mol Pharmacol 65:381–388.

Beier SM, Barish ME (2000) Cholinergic stimulation enhances cytosolic calcium ion accumulation in mouse hippocampal CA1 pyramidal neurones during short action potential trains. J Physiol (Lond) 526[Pt 1]:129–142.

Bland BH, Colom LV, Konopacki J, Roth SH (1988) Intracellular records of carbachol-induced theta rhythm in hippocampal slices. Brain Res 447:364–368.

Blanton MG, Lo Turco JJ, Kriegstein AR (1989) Whole cell recording from neurons in slices of reptilian and mammalian cerebral cortex. J Neurosci Methods 30:203–210.

Breustedt J, Vogt KE, Miller RJ, Nicoll RA, Schmitz D (2003) α_{1E}-containing Ca^{2+} channels are involved in synaptic plasticity. Proc Natl Acad Sci USA 100:12450–12455.

Brown DA, Adams PR (1980) Muscarinic suppression of a novel voltage-sensitive K^+ current in a vertebrate neurone. Nature 283:673–676.

Brown SG, Thomas A, Dekker LV, Tinker A, Leaney JL (2005) PKC-δ sensitizes Kir3.1/3.2 channels to changes in membrane phospholipid levels after M_3 receptor activation in HEK-293 cells. Am J Physiol Cell Physiol 289:C543–C556.

Buzsaki G (2002) Theta oscillations in the hippocampus. Neuron 33:325–340.

Christie BR, Eliot LS, Ito K, Miyakawa H, Johnston D (1995) Different Ca^{2+} channels in soma and dendrites of hippocampal pyramidal neurons mediate spike-induced Ca^{2+} influx. J Neurophysiol 73:2553–2557.

Colino A, Halliwell JV (1993) Carbachol potentiates Q current and activates a calcium-dependent non-specific conductance in rat hippocampus *in vitro*. Eur J Neurosci 5:1198–1209.

Dietrich D, Kirschstein T, Kukley M, Pereverzev A, von der Brelie C, Schneider T, Beck H (2003) Functional specialization of presynaptic $Ca_V2.3$ Ca^{2+} channels. Neuron 39:483–496.

Foehring RC, Mermelstein PG, Song WJ, Ulrich S, Surmeier DJ (2000) Unique properties of R-type calcium currents in neocortical and neostriatal neurons. J Neurophysiol 84:2225–2236.

Fraser DD, MacVicar BA (1996) Cholinergic-dependent plateau potential in hippocampal CA1 pyramidal neurons. J Neurosci 16:4113–4128.

Gahwiler BH, Brown DA (1987) Muscarine affects calcium currents in rat hippocampal pyramidal cells *in vitro*. Neurosci Lett 76:301–306.

Gillies MJ, Traub RD, LeBeau FE, Davies CH, Gloveli T, Buhl EH, Whittington MA (2002) A model of atropine-resistant theta oscillations in rat hippocampal area CA1. J Physiol (Lond) 543:779–793.

Grishin AA, Benquet P, Gerber U (2005) Muscarinic receptor stimulation reduces NMDA responses in CA3 hippocampal pyramidal cells via Ca^{2+}-dependent activation of tyrosine phosphatase. Neuropharmacology 49:328–337.

Halliwell JV, Adams PR (1982) Voltage-clamp analysis of muscarinic excitation in hippocampal neurons. Brain Res 250:71–92.

Huang CS, Shi SH, Ule J, Ruggiu M, Barker LA, Darnell RB, Jan YN, Jan LY (2005) Common molecular pathways mediate long-term potentiation of synaptic excitation and slow synaptic inhibition. Cell 123:105–118.

Huerta PT, Lisman JE (1993) Heightened synaptic plasticity of hippocampal CA1 neurons during a cholinergically induced rhythmic state. Nature 364:723–725.

Huguenard JR (1996) Low-threshold calcium currents in central nervous system neurons. Annu Rev Physiol 58:329–348.

Isomura Y, Fujiwara-Tsukamoto Y, Imanishi M, Nambu A, Takada M (2002) Distance-dependent Ni^{2+} sensitivity of synaptic plasticity in apical dendrites of hippocampal CA1 pyramidal cells. J Neurophysiol 87:1169–1174.

Ito K, Miura M, Furuse H, Zhixiong C, Kato H, Yasutomi D, Inoue T, Mikoshiba K, Kimura T, Sakakibara S (1995) Voltage-gated Ca^{2+} channel blockers, omega-AgaIVA and Ni^{2+}, suppress the induction of theta-burst induced long-term potentiation in guinea-pig hippocampal CA1 neurons. Neurosci Lett 183:112–115.

Kamatchi GL, Franke R, Lynch 3rd C, Sando JJ (2004) Identification of sites responsible for potentiation of type 2.3 calcium currents by acetyl-β-methylcholine. J Biol Chem 279:4102–4109.

Kamondi A, Acsady L, Wang XJ, Buzski G (1998) Theta oscillations in somata and dendrites of hippocampal pyramidal cells *in vivo*: activity-dependent phase-precession of action potentials. Hippocampus 8:244–261.

Klockner U, Lee JH, Cribbs LL, Daud A, Hescheler J, Pereverzev A, Perez-Reyes E, Schneider T (1999) Comparison of the Ca^{2+} currents induced by expression of three cloned α1 subunits, α1G, α1H, and α1I, of low-voltage-activated T-type Ca^{2+} channels. Eur J Neurosci 11:4171–4178.

Kramis R, Vanderwolf CH, Bland BH (1975) Two types of hippocampal rhythmical slow activity in both the rabbit and the rat: relations to behavior and effects of atropine, diethyl ether, urethane, and pentobarbital. Exp Neurol 49:58–85.

Kubota M, Murakoshi T, Saegusa H, Kazuno A, Zong S, Hu Q, Noda T, Tanabe T (2001) Intact LTP and fear memory but impaired spatial memory in mice lacking $Ca_V2.3$ (α_{1E}) channel. Biochem Biophys Res Commun 282:242–248.

Kuzmiski JB, MacVicar BA (2001) Cyclic nucleotide-gated channels contribute to the cholinergic plateau potential in hippocampal CA1 pyramidal neurons. J Neurosci 21:8707–8714.

Kuzmiski JB, MacVicar BA (2003) Muscarinic and metabotropic glutamate receptor enhanced R-type calcium spikes underlie theta oscillations in CA1 pyramidal neurons. Soc Neurosci Abstr 29:258.11.

Kuzmiski JB, Barr W, Zamponi GW, MacVicar BA (2005) Topiramate inhibits the initiation of plateau potentials in CA1 neurons by depressing R-type calcium channels. Epilepsia 46:481–489.

Lee JH, Gomora JC, Cribbs LL, Perez-Reyes E (1999) Nickel block of three

cloned T-type calcium channels: low concentrations selectively block α1H. Biophys J 77:3034–3042.

Leung LW, Yim CY (1991) Intrinsic membrane potential oscillations in hippocampal neurons *in vitro*. Brain Res 553:261–274.

Levey AI, Edmunds SM, Koliatsos V, Wiley RG, Heilman CJ (1995) Expression of M_1–M_4 muscarinic acetylcholine receptor proteins in rat hippocampus and regulation by cholinergic innervation. J Neurosci 15:4077–4092.

Magee JC, Carruth M (1999) Dendritic voltage-gated ion channels regulate the action potential firing mode of hippocampal CA1 pyramidal neurons. J Neurophysiol 82:1895–1901.

Magee JC, Johnston D (1995) Characterization of single voltage-gated Na^+ and Ca^{2+} channels in apical dendrites of rat CA1 pyramidal neurons. J Physiol (Lond) 487 [Pt 1]:67–90.

McNamara RK, Wees EA, Lenox RH (1999) Differential subcellular redistribution of protein kinase C isozymes in the rat hippocampus induced by kainic acid. J Neurochem 72:1735–1743.

Melliti K, Meza U, Adams B (2000) Muscarinic stimulation of α1E Ca channels is selectively blocked by the effector antagonist function of RGS2 and phospholipase C-β1. J Neurosci 20:7167–7173.

Metz AE, Jarsky T, Martina M, Spruston N (2005) R-type calcium channels contribute to afterdepolarization and bursting in hippocampal CA1 pyramidal neurons. J Neurosci 25:5763–5773.

Meza U, Bannister R, Melliti K, Adams B (1999) Biphasic, opposing modulation of cloned neuronal α1E Ca channels by distinct signaling pathways coupled to M_2 muscarinic acetylcholine receptors. J Neurosci 19:6806–6817.

Mogul DJ, Fox AP (1991) Evidence for multiple types of Ca^{2+} channels in acutely isolated hippocampal CA3 neurones of the guinea-pig. J Physiol (Lond) 433:259–281.

Muller W, Connor JA (1991) Cholinergic input uncouples Ca^{2+} changes from K^+ conductance activation and amplifies intradendritic Ca^{2+} changes in hippocampal neurons. Neuron 6:901–905.

Muller W, Connor JA (1992) Ca^{2+} signaling in postsynaptic dendrites and spines of mammalian neurons in brain slice. J Physiol (Paris) 86:57–66.

Naik MU, Benedikz E, Hernandez I, Libien J, Hrabe J, Valsamis M, Dow-Edwards D, Osman M, Sacktor TC (2000) Distribution of protein kinase Mζ and the complete protein kinase C isoform family in rat brain. J Comp Neurol 426:243–258.

Ozawa S, Tsuzuki K, Iino M, Ogura A, Kudo Y (1989) Three types of voltage-dependent calcium current in cultured rat hippocampal neurons. Brain Res 495:329–336.

Perez-Reyes E (2003) Molecular physiology of low-voltage-activated T-type calcium channels [review]. Physiol Rev 83:117–161.

Piedras-Renteria ES, Tsien RW (1998) Antisense oligonucleotides against α1E reduce R-type calcium currents in cerebellar granule cells. Proc Natl Acad Sci USA 95:7760–7765.

Randall AD, Tsien RW (1995) Pharmacological dissection of multiple types of Ca^{2+} channel currents in rat cerebellar granule neurons. J Neurosci 15:2995–3012.

Randall AD, Tsien RW (1997) Contrasting biophysical and pharmacological properties of T-type and R-type calcium channels. Neuropharmacology 36:879–893.

Rouse ST, Marino MJ, Potter LT, Conn PJ, Levey AI (1999) Muscarinic receptor subtypes involved in hippocampal circuits. Life Sci 64:501–509.

Sabatini BL, Svoboda K (2000) Analysis of calcium channels in single spines using optical fluctuation analysis. Nature 408:589–593.

Shapiro MS, Loose MD, Hamilton SE, Nathanson NM, Gomeza J, Wess J, Hille B (1999) Assignment of muscarinic receptor subtypes mediating G-protein modulation of Ca^{2+} channels by using knockout mice. Proc Natl Acad Sci USA 96:10899–10904.

Shapiro MS, Gomeza J, Hamilton SE, Hille B, Loose MD, Nathanson NM, Roche JP, Wess J (2001) Identification of subtypes of muscarinic receptors that regulate Ca^{2+} and K^+ channel activity in sympathetic neurons. Life Sci 68:2481–2487.

Sochivko D, Pereverzev A, Smyth N, Gissel C, Schneider T, Beck H (2002) The Ca_V2.3 Ca^{2+} channel subunit contributes to R-type Ca^{2+} currents in murine hippocampal and neocortical neurones. J Physiol (Lond) 542:699–710.

Sochivko D, Chen J, Becker A, Beck H (2003) Blocker-resistant Ca^{2+} currents in rat CA1 hippocampal pyramidal neurons. Neuroscience 116:629–638.

Stea A, Soong TW, Snutch TP (1995) Determinants of PKC-dependent modulation of a family of neuronal calcium channels. Neuron 15:929–940.

Stewart AE, Yan Z, Surmeier DJ, Foehring RC (1999) Muscarine modulates Ca^{2+} channel currents in rat sensorimotor pyramidal cells via two distinct pathways. J Neurophysiol 81:72–84.

Talley EM, Cribbs LL, Lee JH, Daud A, Perez-Reyes E, Bayliss DA (1999) Differential distribution of three members of a gene family encoding low voltage-activated (T-type) calcium channels. J Neurosci 19:1895–1911.

Tang FR, Lee WL, Gao H, Chen Y, Loh YT, Chia SC (2004) Expression of different isoforms of protein kinase C in the rat hippocampus after pilocarpine-induced status epilepticus with special reference to CA1 area and the dentate gyrus. Hippocampus 14:87–98.

Tsubokawa H, Ross WN (1997) Muscarinic modulation of spike back-propagation in the apical dendrites of hippocampal CA1 pyramidal neurons. J Neurosci 17:5782–5791.

Vilaro MT, Mengod G, Palacios G, Palacios JM (1993) Receptor distribution in the human and animal hippocampus: focus on muscarinic acetylcholine receptors. Hippocampus 3[Spec No]:149–156.

Wilson SM, Toth PT, Oh SB, Gillard SE, Volsen S, Ren D, Philipson LH, Lee EC, Fletcher CF, Tessarollo L, Copeland NG, Jenkins NA, Miller RJ (2000) The status of voltage-dependent calcium channels in α_{1E} knockout mice. J Neurosci 20:8566–8571.

Yasuda R, Sabatini BL, Svoboda K (2003) Plasticity of calcium channels in dendritic spines. Nat Neurosci 6:948–955.

Yunker AM (2003) Modulation and pharmacology of low voltage-activated ("T-type") calcium channels. J Bioenerg Biomembr 35:577–598.

Zhang JF, Randall AD, Ellinor PT, Horne WA, Sather WA, Tanabe T, Schwarz TL, Tsien RW (1993) Distinctive pharmacology and kinetics of cloned neuronal Ca^{2+} channels and their possible counterparts in mammalian CNS neurons. Neuropharmacology 32:1075–1088.

Zhao W, Bianchi R, Wang M, Wong RK (2004) Extracellular signal-regulated kinase 1/2 is required for the induction of group I metabotropic glutamate receptor-mediated epileptiform discharges. J Neurosci 24:76–84.